Bio-Adhesive Nanoporous Module: Toward Autonomous Gating

Hyuna Jo,[a] Takashi Kitao,[d] Ayumi Kimura,[e] Yoshimitsu Itoh,[a] Takuzo Aida,*[a][c] and Kou Okuro*[a][b]

[a] H. Jo, Dr. Y. Itoh, Prof. Dr. T. Aida, Dr. K. Okuro
Department of Chemistry and Biotechnology, School of Engineering
The University of Tokyo
7-3-1 Hongo, Bunkyo-ku, Tokyo 113-8656 (Japan)
E-mail: aida@macro.t.u-tokyo.ac.jp
okuro@hku.hk
[b] Dr. K. Okuro
Department of Chemistry, The University of Hong Kong
Pokfulam Road, Hong Kong (China)
[c] Prof. Dr. T. Aida
RIKEN Center for Emergent Matter Science
2-1 Hirosawa, Wako, Saitama 351-0198 (Japan)
[d] Dr. T. Kitao
Department of Advanced Materials Science, Graduate School of Frontier Sciences and Department of Applied Chemistry, Graduate School of Engineering,
The University of Tokyo
Chiba 227-8561 (Japan)
[e] A. Kimura
Institute of Engineering Innovation, The University of Tokyo
2-11-16 Yayoi, Bunkyo-ku, Tokyo 113-8656 (Japan)

Abstract: Here we report a bio-adhesive porous organic module (^{Glue}COF) composed of hexagonally packed 1D nanopores based on a covalent organic framework. The nanopores are densely appended with guanidinium ion (Gu^+) pendants capable of salt-bridging with oxyanionic species. Because oxyanionic species are ubiquitously present in biopolymers, ^{Glue}COF strongly adheres to biopolymers via a multivalent salt-bridging interaction. By taking advantage of its strong bio-adhesive nature, we succeeded in creating a gate that possibly opens the nanopores via a selective interaction with a reporter chemical and releases guest molecules. We chose calmodulin (CaM) as a gating component that can stably entrap a loaded guest, sulforhodamine B (SRB), within the nanopores (^{CaM}COF⊃SRB). CaM is known to change its conformation via selective binding with Ca^{2+}. We confirmed that, upon mixing with Ca^{2+}, ^{CaM}COF⊃SRB released SRB from its nanopores, whereas the use of weakly binding Mg^{2+} resulted in much slower release of SRB.

Introduction

Stimuli-responsive guest release is one of the important functions of porous materials.[1] So far, a wide variety of inorganic and organic porous materials with a photo-responsive gating mechanism have been developed by attaching azobenzene derivatives to the pore exits.[2–5] This mechanism is promising, if the light exposure is not physically interfered, and the pores are relatively small. Apart from such a manual gating mechanism, autonomous gating that would ideally enable opening and closing motions of the gate in response to the concentration change of a reporter chemical has also attracted great attention.[2–7] One of possible strategies toward autonomous gating would be to utilize a protein as the gating component that possibly changes its conformation through selective binding with a reporter chemical. This strategy is also advantageous, because a large-dimension protein, if any appropriate is available for this purpose, would be applicable to porous materials with large pores. However, despite its great potential, autonomous gating via chemically induced conformational changes of proteins has rarely been explored.

Here we report ^{Glue}COF (Figure 1) that is a bio-adhesive porous organic module enabling the adhesion-based attachment of calmodulin (CaM) as a gate (Figure 2). Its porous scaffold employed the basic architecture of an imine-based covalent organic framework (COF).[8,9] As shown in Figure 1, the nanopores of ^{Glue}COF are densely functionalized with a large number of guanidinium ion (Gu^+) pendants[10] that can be salt-bridged with the oxyanionic surface groups of biopolymers.[11] Oxyanions exist ubiquitously in proteins and nucleic acids as well as on metal oxide surfaces. Therefore, we thought that ^{Glue}COF could adhere to CaM via a multivalent salt-bridging interaction.[11,12] Why did we choose CaM? This protein is known to change its conformation via selective binding with Ca^{2+} (K_d = 0.1–1.0 μM).[13] We ambitioned that CaM in ^{CaM}COF⊃guest, when it binds to Ca^{2+}, may undergo a Ca^{2+}-induced conformational change that allows the guest molecules to be released from the nanopores. Meanwhile, Ca^{2+} is an important biological reporter for bone diseases such as multiple myeloma,[13] where the local

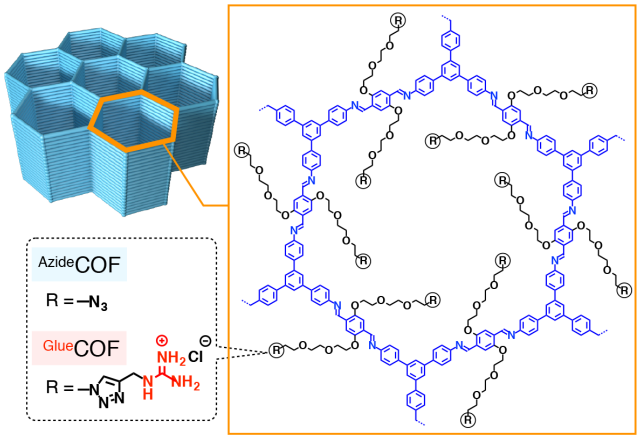

Figure 1. Molecular structures of porous organic modules ^{Azide}COF and ^{Glue}COF bearing azide (N_3) and guanidinium ion (Gu^+) pendants, respectively.

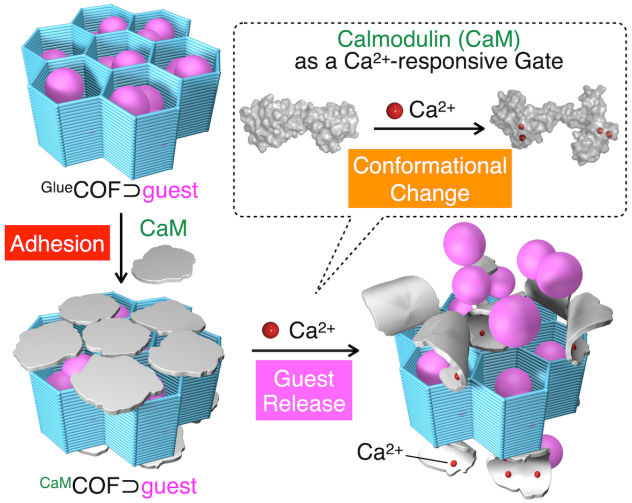

Figure 2. Schematic illustration of Ca^{2+}-responsive guest release from ^{CaM}COF⊃guest, whose guest-loaded nanopores are blocked by calmodulin (CaM) as a gate. First, guest molecules are loaded into the nanopores of ^{Glue}COF. ^{Glue}COF⊃guest, thus obtained, was allowed to adhere to CaM through a multivalent salt-bridging interaction (^{CaM}COF⊃guest). Upon binding with Ca^{2+}, the CaM gate in ^{CaM}COF⊃guest changes its conformation for guest release.

concentrations of Ca^{2+} at diseased sites are usually higher than 4 mM.[14]

Results and Discussion

For obtaining ^{Glue}COF (Figure 1), we first synthesized azide-appended ^{Azide}COF (Figure 1) by a method analogous to that reported previously,[15] and subjected to a Cu(I)-catalyzed azide–alkyne "click" reaction[16] with propargyl guanidine (PG) at [PG]/[-N_3] = 1.2 in THF/water (*v*/*v* = 3/1) for 4 h (Figure 3a). In X-ray photoelectron spectroscopy (XPS), the reaction mixture (^{Glue}COF; Figure 3b, red) showed a broad peak in a range from 396 eV to 403 eV, which is most likely composed of peaks due to triazole (TAZ; 399.5 and 400.7 eV),[17] Gu^+ (398.9 eV),[18] and C=N (397.9 eV).[19] A peak due to -N_3 (central nitrogen; 403.4 eV),[20] which was clearly observed for precursor ^{Azide}COF (Figure 3b, blue), did not appear after the azide–alkyne "click" reaction. In Fourier-transform infrared (FT-IR) spectroscopy, the reaction mixture (^{Glue}COF; Figure 3c, red) showed N-H stretching vibrations at 3163 and 3371 cm^{-1} due to Gu^+ and a C=N stretching vibration at 1672 cm^{-1} due to TAZ,[21] at the expense of the -N_3 stretching vibration at 2107 cm^{-1}, which was clearly observed for precursor ^{Azide}COF (Figure 3c, blue).[21] Solid-state ^{13}C NMR spectroscopy of the reaction mixture (^{Glue}COF; Figure 3d, red) showed the appearance of new signals due to TAZ-*C*H_2-Gu^+ at 37.1 ppm (signal *l*; Figures S4 and S6 for model compounds)[22] and Gu^+ at 159.1 ppm (signal a; Figures S4 and S6),[22] which were not observed for precursor ^{Azide}COF (Figure 3d, blue). The integral ratio of signal *l* versus signal TEG' allowed for estimating the conversion of ^{Azide}COF into ^{Glue}COF as 82%. As confirmed by XPS (Figure S7)[22] and inductively coupled plasma atomic emission spectroscopy (ICP-AES; Table S1), the amount of residual Cu in ^{Glue}COF was negligibly small (0.0011 wt%) when washed with THF and an aqueous EDTA solution (0.01 M). Furthermore, powder X-ray diffraction (PXRD) patterns of

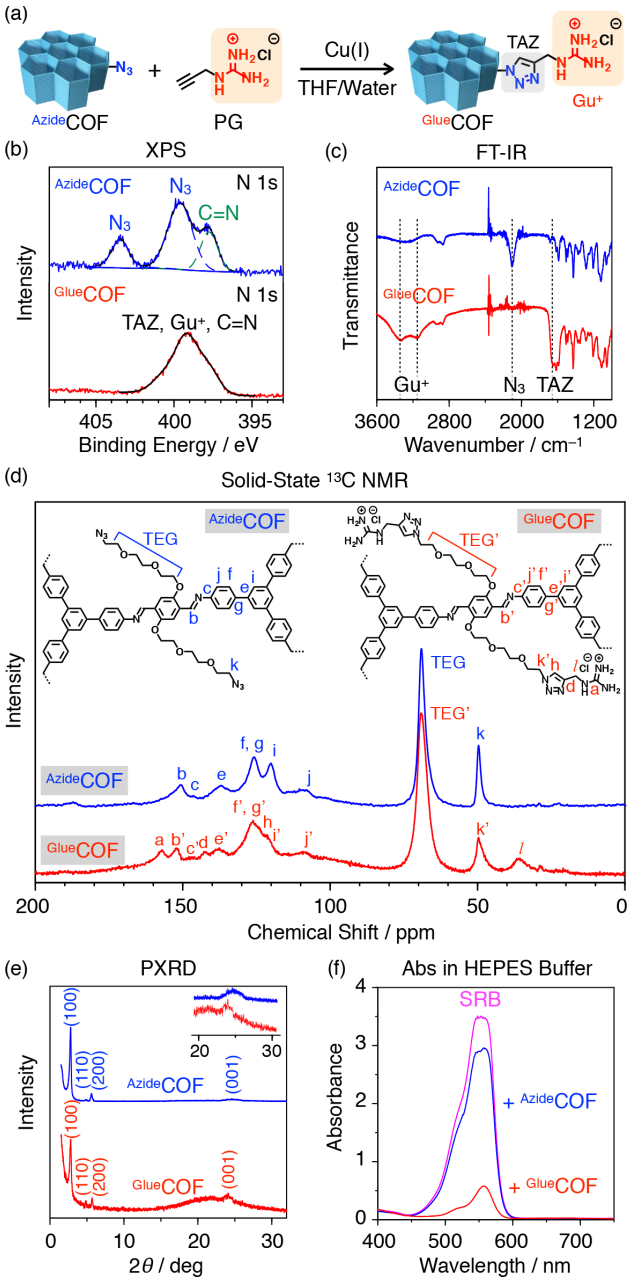

Figure 3. (a) Synthesis of ^{Glue}COF by a Cu(I)-catalyzed azide-alkyne "click" reaction between ^{Azide}COF and propargyl guanidine (PG). (b) X-ray photoelectron spectroscopy (XPS) of ^{Azide}COF (blue) and its "click" reaction mixture (^{Glue}COF, red). (c) Fourier-transform infrared (FT-IR) spectra of ^{Azide}COF (blue) and its "click" reaction mixture (^{Glue}COF, red). (d) Solid-state ^{13}C NMR spectra of ^{Azide}COF (blue) and its "click" reaction mixture (^{Glue}COF, red). (e) Powder X-ray diffraction (PXRD) patterns of ^{Azide}COF (blue) and its "click" reaction mixture (^{Glue}COF, red). The inset shows magnified profiles at 20°–30° in 2θ. (f) Absorption spectra of an aqueous solution of sulforhodamine B (SRB, 50 μM) before (pink) and after mixing with ^{Azide}COF (100 μg mL^{-1}, blue) and ^{Glue}COF (100 μg mL^{-1}, red).

^{Azide}COF and its "click" reaction mixture (^{Glue}COF) both showed diffraction peaks characteristic of a 2D hexagonal geometry[9] at 2θ = 2.90°, 4.86°, 5.76°, and 24.6° (Figure 3e), which could be indexed as (100), (110), (200), and (001), respectively, based on their simulated patterns (Figure S8).[22] By Pawley refinement, we calculated the unit cell parameters of ^{Glue}COF as *a* = *b* = 34.91 Å

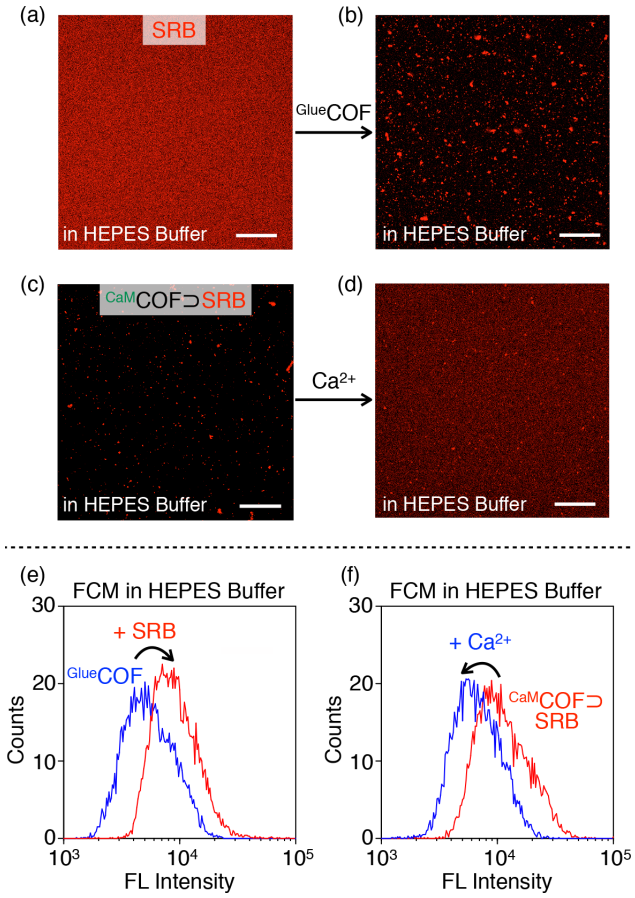

Figure 4. (a, b) Confocal laser scanning microscopy (CLSM; λ_{ex} = 550 nm, λ_{obs} = 560–620 nm) images of a HEPES (20 mM, pH 7.2) buffer solution of SRB (1 μM) before (a) and (b) after 3-h incubation with ^{Glue}COF⊃none (100 μg mL^{-1}). Scale bars = 20 μm. (c, d) CLSM images of a HEPES (20 mM, pH 7.2) buffer suspension of ^{CaM}COF⊃SRB ([^{Glue}COF] = 5 μg mL^{-1}, [SRB] = 1.6 μM) before (c) and (d) after 48-h incubation with Ca^{2+} ([$CaCl_2$ = 8 mM]). Scale bars = 20 μm. (e, f) Flow cytometry (FCM) histograms (λ_{ex} = 488 nm) of a HEPES (20 mM, pH 7.2) buffer suspension of (e) ^{Glue}COF before (blue) and after 3-h incubation with SRB (1 μM, blue → red), and (f) ^{CaM}COF⊃SRB before and after 48-h incubation with Ca^{2+} ([$CaCl_2$ = 8 mM], blue → red).

and c = 4.25 Å. The transmission electron microscopy (TEM) of ^{Glue}COF showed a power spectrum characteristic of hexagonally packed 1D pores (Figure S9).[22] Atomic force microscopy (AFM) showed that the ^{Glue}COF particles were 20–80 nm thick (Figure S11).[22] Of interest, its Brunauer-Emmett-Teller (BET) surface area (46 m^2 g^{-1}; Figure S12)[22] was much smaller than that of its precursor ^{Azide}COF (366 m^2 g^{-1}; Figure S12).[22] Considering the highly hygroscopic nature of Gu$^+$, the ^{Glue}COF nanopores are likely filled with water. In fact, thermogravimetric analysis (TGA) of ^{Glue}COF clearly showed a weight loss at 25–100 °C (Figure S13),[22] from which the number of water molecules per COF unit cell was estimated as ~9. This value agreed well with the result of elemental analysis (Table S1).[22]

By means of confocal laser scanning microscopy (CLSM; λ_{ex} = 552 nm), we confirmed that ^{Glue}COF⊃none was able to trap sulforhodamine B (SRB; sodium salt), a negatively charged fluorescent dye with an estimated size of 1.6 nm × 1.2 nm.[23] Although a HEPES buffer (20 mM, pH 7.2) solution of SRB showed a bright fluorescence (Figure 4a), it gradually became dark upon addition of ^{Glue}COF⊃none (Figure 4b). At the same time, the ^{Glue}COF particles became fluorescent. Accordingly, in flow cytometry (FCM; λ_{ex} = 488 nm), ^{Glue}COF⊃SRB, as expected, emitted more intense fluorescence (Figure 4e, red) than ^{Glue}COF (Figure 4e, blue). Note that the ^{Glue}COF particles, suspended in an aqueous medium, gradually aggregate and eventually precipitate. By virtue of this precipitation behavior, we quantitatively evaluated the guest loading capacity of ^{Glue}COF using SRB as the guest. Thus, a suspension of ^{Glue}COF (100 μg mL^{-1}) was added to an aqueous solution of SRB (50 μM; Figure 3f, pink) at 25 °C, and the resulting suspension, after being stirred for 3 h, was allowed to stand for 1 h, whereupon a precipitate formed. Its supernatant portion obviously showed a smaller SRB absorption at 550–570 nm than that before the addition of ^{Glue}COF (Figure 3f, red). Based on this spectral change, the loading capacity of ^{Glue}COF for SRB was evaluated as 18 wt% (0.87 SRB molecules per COF unit cell; 0.17 SRB molecules per Gu$^+$ pendant),[22] which is comparable to those reported for other COFs (9.7–32.5 wt%).[8] We created an energy-minimized computational model of ^{Glue}COF having 1.8 nm-diameter nanopores (Figure S36),[22] which are large enough to accommodate one molecule of SRB in consistency with the loading capacity of ^{Glue}COF for SRB.

Despite the small BET surface area possibly due to a hygroscopic nature of its nanopores, ^{Glue}COF showed such a satisfactorily large loading capacity for SRB, suggesting that the water molecules, initially solvating the Gu$^+$ pendants in the nanopores, were replaced with salt-bridge-formable SRB carrying two sulfonate (SO_4^{2-}) groups. In sharp contrast, ^{Azide}COF with no Gu$^+$ pendants barely trapped SRB (Figure 3f, blue; estimated

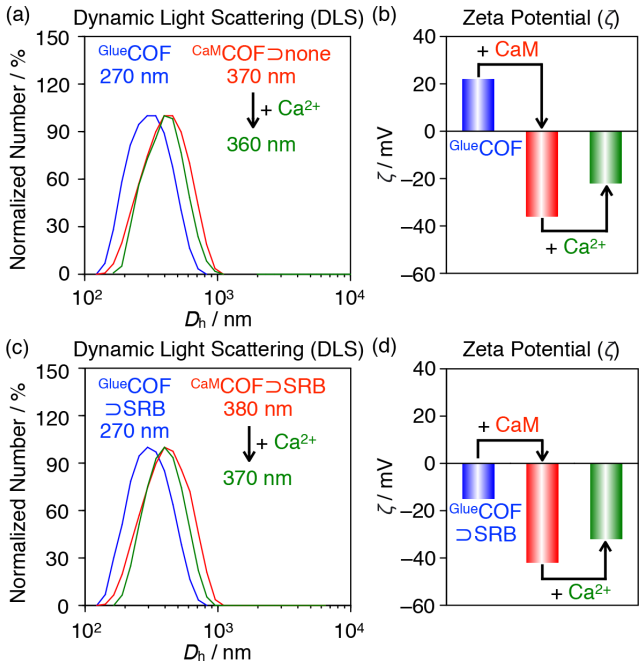

Figure 5. (a, c) Histograms of the dynamic light scattering (DLS) data at 25 °C in HEPES buffer solutions (20 mM, pH 7.2) of (a) guest-free ^{Glue}COF before and after mixing with CaM (blue → red) followed by Ca^{2+} ([$CaCl_2$] = 8 mM, green), and (c) SRB-loaded ^{Glue}COF before (^{Glue}COF⊃SRB) and after mixing with CaM (blue → red) followed by Ca^{2+} (green). (b, d) Zeta potential values at 25 °C in HEPES buffer solutions (20 mM, pH 7.2) of (b) guest-free ^{Glue}COF before and after mixing with CaM (blue → red) followed by Ca^{2+} (green), and (d) SRB-loaded ^{Glue}COF before (^{Glue}COF⊃SRB) and after mixing with CaM (blue → red), followed by Ca^{2+} (green).

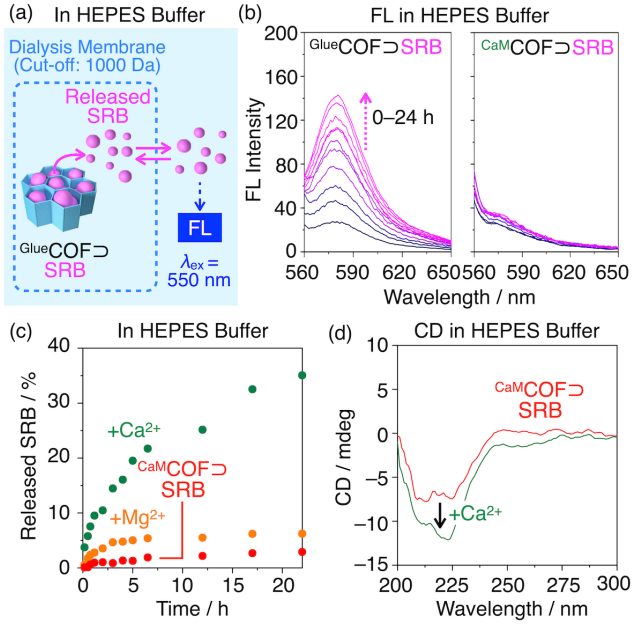

Figure 6. (a) Schematic illustration of the experimental setup for guest release from ^{Glue}COF⊃SRB. Typically, a HEPES (20 mM, pH 7.2) buffer suspension (100 μL) of ^{Glue}COF⊃SRB ([^{Glue}COF] = 5 μg mL^{-1}, [SRB] = 1.6 μM) is transferred to a dialysis tube with a semi-permeable membrane (cutoff: 1000 Da) and incubated in HEPES buffer at 37 °C. SRB (molecular weight: 558.6 g mol^{-1}) is released from ^{Glue}COF⊃SRB and passes through the membrane, whereas ^{Glue}COF⊃SRB (D_h = 270 nm) stays inside the dialysis tube. The released SRB is quantified based on the fluorescence intensity of the solution outside the dialysis tube. (b) Fluorescence spectral changes (λ_{ex} = 550 nm) outside the dialysis tube containing the suspensions of ^{Glue}COF⊃SRB and ^{CaM}COF⊃SRB ([CaM] = 1 mM). (c) SRB release profiles of ^{CaM}COF⊃SRB ([CaM] = 1 mM, [^{Glue}COF] = 5 μg mL^{-1}) in the absence (red) and presence of Ca^{2+} ([$CaCl_2$] = 8 mM; green) and Mg^{2+} ([$MgCl_2$] = 8 mM; orange). (d) Circular dichroism (CD) spectra of a HEPES (20 mM, pH 7.2) buffer suspension of ^{CaM}COF⊃SRB ([^{Glue}COF] = 0.5 μg mL^{-1}, [SRB] = 0.1 μM, [CaM] = 50 μM) before and after mixing with Ca^{2+} (red → green).

loading capacity ~2.4 wt%), although its BET surface area was 9 times larger than that of ^{Glue}COF.

Next, we examined whether CaM indeed adheres to ^{Glue}COF or not. Dynamic light scattering (DLS) analysis in HEPES buffer (20 mM, pH 7.2) showed that, after mixing with CaM (1 mM; D_h = 4 nm; Figure S24), ^{Glue}COF (5 μg mL^{-1}; D_h = 270 nm) and ^{Glue}COF⊃SRB ([^{Glue}COF] = 5 μg mL^{-1}, [SRB] = 1.6 μM) both increased their hydrodynamic diameters (Figure 5a and 5c, blue → red). Furthermore, the zeta potentials (ζ) of both ^{Glue}COF (ζ = +22 mV) and ^{Glue}COF⊃SRB (ζ = –16 mV) were negatively increased after mixing with CaM (Figure 5b and 5d, blue → red). These results are reasonable, considering that CaM is a negatively charged protein (ζ = –61 mV; Figure S27).[22] Namely, CaM adheres to the surface of both ^{Glue}COF and ^{Glue}COF⊃SRB. After the adhesion, CaM blocks the nanopores and protect included guests. For example, as confirmed by CLSM, ^{CaM}COF⊃none could not trap SRB, even though it was guest-free (Figure S33).[22] Sodium dithionite ($Na_2S_2O_4$) is known to reductively degrade SRB and quench its fluorescence.[24] So, we investigated whether SRB in ^{Glue}COF⊃SRB and ^{CaM}COF⊃SRB ([CaM] = 1 mM) are protected against $Na_2S_2O_4$. As shown in Figure S23a, when a HEPES buffer suspension of ^{Glue}COF⊃SRB was titrated with $Na_2S_2O_4$, the SRB fluorescence at 580 nm was quenched significantly. In contrast, ^{CaM}COF⊃SRB with a CaM gate ([CaM] = 1 mM), under identical conditions, dropped its fluorescence intensity only in the initial stage of titration (Figure S23b). Thus, we conclude that CaM properly serves as the gate for the nanopores to physically protect included SRB against reduction.

As described in the introductory part, CaM is a highly potent protein as a stimuli-responsive gating unit. At first, we investigated how rapidly non-blocked ^{Glue}COF⊃SRB releases SRB. Thus, a HEPES (20 mM, pH 7.2) buffer suspension (100 μL) of ^{Glue}COF⊃SRB ([^{Glue}COF] = 5 μg mL^{-1}, [SRB] = 1.6 μM) was transferred to a dialysis tube with a semi-permeable membrane (cutoff: 1000 Da) that allowed released SRB to pass through, and then incubated at 37 °C (Figure 6a). As shown in Figure 6b, a fluorescence band at 580 nm (λ_{ex} = 550 nm) due to leaked SRB emerged in the HEPES buffer solution located outside the dialysis tube. In 24 h, the amount of leaked SRB reached 42% of the initially loaded SRB (Figure S18, blue).[22] As expected, when ^{Glue}COF⊃SRB was converted beforehand into ^{CaM}COF⊃SRB using CaM (1 mM), the amount of leaked SRB upon incubation was negligibly small (Figures 6b and 6c, red). Then, what would happen upon mixing with Ca^{2+}? When Ca^{2+} ([$CaCl_2$] = 8 mM) was added to the HEPES buffer suspension of ^{CaM}COF⊃SRB, the release of SRB started (Figures 6c, green, and S16a).[22] Accordingly, the liquid phase of the ^{CaM}COF⊃SRB suspension became entirely fluorescent, as confirmed by CLSM (Figures 4c and 4d). The release of SRB was also supported by FCM (Figure 4f), where ^{CaM}COF⊃SRB became much less fluorescent. Note that, upon mixing with Ca^{2+} (D_h = 360 nm; Figure 5a, green), ^{CaM}COF⊃SRB barely changed its hydrodynamic diameter D_h (Figure 5b, red → green), its zeta-potential ζ positively increased from –36 mV to –22 mV (Figure 5d, red → green). We also confirmed that ^{CaM}COF⊃SRB ([^{Glue}COF] = 0.5 μg mL^{-1}, [CaM] = 50 μM), upon mixing with Ca^{2+} ([$CaCl_2$] = 8 mM), changed its circular dichroism (CD) spectrum (Figure 6d), which is analogous to that observed for CaM alone (Figure S28).[13b,13c,22] From the release rates at different [Ca^{2+}] (Figures S19 and S20),[22] the half maximal effective concentration (EC_{50}) of Ca^{2+} for the SRB release was estimated as 14 mM (Figure S21).[22] Under identical conditions, the EC_{50} value of Ca^{2+} for the conformational change of CaM, as estimated from the CD spectral titration of ^{CaM}COF⊃SRB (Figure S29),[22] was 9.4 mM (Figure S30),[22] which is in good agreement with the EC_{50} value of Ca^{2+} for the SRB release. Therefore, the release of SRB is most likely caused by the Ca^{2+}-induced conformational change of CaM. As a control, we investigated the release of SRB from a mixture of CaM and ^{Azide}COF as a non-adhesive version of ^{Glue}COF and confirmed that the nanopores rapidly released SRB even without Ca^{2+} (Figure S22),[22] indicating that the CaM does not serve as a gate for ^{Azide}COF lacking adhesive Gu^{+} pendants.

Different from Ca^{2+}, Mg^{2+} interacts with CaM only weakly.[13d] Accordingly, when Mg^{2+} ([$MgCl_2$] = 8 mM), instead of Ca^{2+}, was mixed with ^{CaM}COF⊃SRB in a HEPES buffer suspension, the release of SRB from the nanopores occurred much less efficiently (Figure 6c, orange, and S16b).[22] We also found that bovine serum albumin (BSA; D_h = 6 nm, Figure S24),[22] analogous to CaM, can block the SRB-loaded nanopores of ^{Glue}COF⊃SRB (Figures S15 and S18).[22] However, as expected, mixing of ^{BSA}COF⊃SRB ([^{Glue}COF] = 5 μg mL^{-1}, [BSA] = 1 mM, [SRB] = 1.6 μM) with Ca^{2+} ([$CaCl_2$] = 8 mM) did not result in the release of SRB (Figure S17).[22] Of interest, ^{CaM}COF⊃SRB was revealed to enter live cells (Figure S34)[22] without appreciable cytotoxicity (Figure S35).[22]

Conclusions

As a proof-of-concept study on the development of nanoporous modules with an autonomous gating mechanism, we have shown that our newly developed bio-adhesive ^{Glue}COF with hexagonally packed Gu^{+}-appended nanopores, has the large potential for this direction. When a particular protein such as calmodulin (CaM) is allowed to adhere to ^{Glue}COF as the gating component, ^{CaM}COF undergoes a large conformational change when bound with Ca^{2+}, a reporter chemical. We confirmed that ^{CaM}COF successfully releases a guest such as SRB from its nanopores in response to Ca^{2+}. As a future perspective, it is important to extend the range of biopolymers as candidates for gating components to respond to a wider variety of stimuli. Even more challenging is to apply bio-adhesive ^{Glue}COF to other biological motifs such as living cells, which is one of the subjects worthy of further investigation.

Acknowledgements

This work was supported by Seed Fund for Basic Research for New Staff of the University of Hong Kong (201909185032) and General Research Fund (GRF) from the Research Grants Council of Hong Kong (17304320) to K.O., and partially supported by Grant-in-Aid for Scientific Research (S) (18H05260) to T.A. H. J. thanks the Research Fellowship of Japan Society for the Promotion of Science (JSPS) for Young Scientists. We appreciate Prof. H. Cabral (The University of Tokyo) for zeta-potential measurements. We are grateful to the materials characterization support team, RIKEN Center for Emergent Matter Science for the elemental analysis.

Keywords: adhesive materials • porous materials • gating phenomena • host-guest chemistry

[1] a) K. E. Uhrich, S. M. Cannizzaro, R. S. Langer, K. M. Shakesheff, *Chem. Rev.* **1999**, *99*, 3181–3198; b) I. I. Slowing, J. L. Vivero-Escoto, C. W. Wu, V. S.-Y. Lin, *Adv. Drug Delivery Rev.* **2008**, *60*, 1278–1288; (c) H. K. Makadia, S. J. Siegel, *Polymers* **2011**, *3*, 1377–1397; (d) S. Mura, J. Nicolas, P. Couvreur, *Nat. Mater.* **2013**, *12*, 991–1003; (e) N. Kamaly, B. Yameen, J. Wu, O. C. Farokhzad, *Chem. Rev.* **2016**, *116*, 2602–2663.

[2] a) Q. Fu, G. V. R. Rao, L. K. Ista, Y. Wu, B. P. Andrzejewski, L. A. Sklar, T. L. Ward, G. P. López, *Adv. Mater.* **2003**, *15*, 1262–1266; b) R. Hernandez, H.-R. Tseng, J. W. Wong, J. F. Stoddart, J. I. Zink, *J. Am. Chem. Soc.* **2004**, *126*, 3370−3371; c) Y. Zhu, M. Fujiwara, *Angew. Chem., Int. Ed.* **2007,** *46*, 2241–2244; *Angew. Chem*. **2007**, *119*, 2291–2294; d) J. Lu, E. Choi, F. Tamanoi, J. I. Zink, *Small* **2008**, *4*, 421–426; e) A. F. Moreira, D. R. Dias, I. J. Correia, *Microporous Mesoporous Mater.* **2016**, *236*, 141–157; f) C.-A. Cheng, T. Deng, F.-C. Lin, Y. Cai, J. I. Zink, *Theranostics* **2019**, *9*, 3341–3364.

[3] S. Zhu, C. Chen, Z. Chen, X. Liu, Y. Li, Y. Shi, D. Zhang, *Mater. Chem. Phys.* **2011**, *126*, 357–363.

[4] a) S. Tang, X. Huang, X. Chen, N. Zheng, *Adv. Funct. Mater.* **2010**, *20*, 2442–2447; b) M. D. Wang, G. C. Gong, J. Feng, T. Wang, C. D. Ding, B. J. Zhou, W. Jiang, J. J. Fu, *ACS Appl. Mater. Interfaces* **2016**, *8*, 23289–23301.

[5] a) J. W. Brown, B. L. Henderson, M. D. Kiesz, A. C. Whalley, W. Morris, S. Grunder, H. Deng, H. Furukawa, J. I. Zink, J. F. Stoddart, O. M. Yaghi, *Chem. Sci.* **2013**, *4*, 2858–2864; b) S. Nagata, K. Kokado, K. Sada, *Chem. Commun.* **2015**, *51*, 8614–8617; c) L.-L. Tan, N. Song, S. X.-A. Zhang, H. Li, B. Wang, Y.-W. Yang, *J. Mater. Chem. B* **2016**, *4*, 135–140; d) X. Meng, B. Gui, D. Yuan, M. Zeller, C. Wang, *Sci. Adv.* **2016**, *2*, e1600480.

[6] E. Aznar, M. Oroval, L. Pascual, J. R. Murguía, R. Martínez-Máñez, F. Sancenón, *Chem. Rev.* **2016**, *116*, 561–718.

[7] a) V. C. Özalp, T. Schäfer, *Chem. Eur. J.* **2011**, *17*, 9893–9896; b) D. He, X. He, K. Wang, J. Cao, Y. Zhao, *Adv. Funct. Mater.* **2012**, *22*, 4704–4710.

[8] a) Q. Fang, J. Wang, S. Gu, R. B. Kaspar, Z. Zhuang, J. Zheng, H. Guo, S. Qiu, Y. Yan, *J. Am. Chem. Soc.* **2015**, *137*, 8352–8355; b) S. Kandambeth, V. Venkatesh, D. B. Shinde, S. Kumari, A. Halder, S. Verma, R. Banerjee, *Nat. Commun.* **2015**, *6*, 6786; c) L. Bai, S. Z. F. Phua, W. Q. Lim, A. Jana, Z. Luo, H. P. Tham, L. Zhao, Q. Gao, Y. Zhao, *Chem. Commun.* **2016**, *52*, 4128–4131; d) D. Liu, W. Zhang, Q. Zeng, S. A. Lei, *Chem. Eur. J.* **2016**, *22*, 6768–6773; e) V. S. Vyas, M. Vishwakarma, I. Moudrakovski, F. Haase, G. Savasci, C. Ochsenfeld, J. P. Spatz, B. V. Lotsch, *Adv. Mater.* **2016**, *28*, 8749–8754; f) S. Mitra, H. S. Sasmal, T. Kundu, S. Kandambeth, K. Illath, D. D. Diaz, R. Banerjee, *J. Am. Chem. Soc.* **2017**, *139*, 4513–4520; g) G. Zhang, X. Li, Q. Liao, Y. Liu, K. Xi, W. Huang, X. Jia, *Nat. Commun.* **2018**, *9*, 2785; h) S. Liu, C. Hu, Y. Liu, X. Zhao, M. Pang, J. Lin, *Chem. Eur. J.* **2019**, *25,* 4315–4319; i) Q. Guan, L.-L. Zhou, F.-H. Lv, W.-Y. Li, Y.-A. Li, Y.-B. Dong, *Angew. Chem. Int. Ed.* **2020**, *59*, 18042–18047; *Angew. Chem.* **2020**, *132*, 18198–18203.

[9] M. Matsumoto, R. R. Dasari, W. Ji, C. H. Feriante, T. C. Parker, S. R. Marder, W. R. Dichtel, *J. Am. Chem. Soc.* **2017**, *139*, 4999–5002.

[10] a) N. Sakai, S. Matile, *J. Am. Chem. Soc.* **2003**, *125*, 14348–14356; b) A. Hennig, G. J. Gabriel, G. N. Tew, S. Matile, *J. Am. Chem. Soc.* **2008**, *130*, 10338–10344; c) D. Shukla, C. P. Schneider, B. L. Trout, *J. Am. Chem. Soc.* **2011**, *133*, 18713–18718; d) E. I. Geihe, C. B. Cooley, J. R. Simon, M. K. Kiesewetter, J. A. Edward, R. P. Hickerson, R. L. Kaspar, J. L. Hedrick, R. M. Waymouth, P. A. Wender, *Proc. Natl. Acad. Sci. U. S. A.* **2012**, *109*, 13171–13176; e) E.-K. Bang, G. Gasparini, G. Molinard, A. Roux, N. Sakai, S. Matile, *J. Am. Chem. Soc.* **2013**, *135*, 2088–2091; f) G. Gasparini, E. -K. Bang, G. Molinard, D. V. Tulumello, S. Ward, S. O. Kelley, A. Roux, N. Sakai, S. Matile, *J. Am. Chem. Soc.* **2014**, *136*, 6069–6074; g) G. Gasparini, S. Matile, *Chem. Commun.* **2015**, *51*, 17160−17162; h) C. J. McKinlay, R. M. Waymouth, P. A. Wender, *J. Am. Chem. Soc.* **2016**, *138*, 3510–3517; i) E. Derivery, E. Bartolami, S. Matile, M. Gonzalez-Gaitan, *J. Am. Chem. Soc.* **2017**, *139*, 10172–10175.

[11] R. Mogaki, P. K. Hashim, K. Okuro, T. Aida, *Chem. Soc. Rev.* **2017**, *46*, 6480–6491.

[12] a) K. Okuro, K. Kinbara, K. Tsumoto, N. Ishii, T. Aida, *J. Am. Chem. Soc.* **2009**, *131*, 1626−1627; b) R. Mogaki, K. Okuro, R. Ueki, S. Sando, T. Aida, *J. Am. Chem. Soc.* **2019**, *141*, 8035–8040; c) N. B. Hentzen, R. Mogaki, S. Otake, K. Okuro, T. Aida, *J. Am. Chem. Soc.*, **2020**, *142*, 8080–8084.

[13] a) T. Ozawa, K. Sasaki, Y. Umezawa, *Biochim. Biophys. Acta*, **1999**, *1434*, 211–220; b) L. Settimoto, S. Donnini, A. H. Juffer, R. W. Woody, O. Marin, *Pept. Sci.* **2006**, *88*, 373–385; c) Y. Zhou, W. Yang, M. M. Lurtz, Y. Ye, Y. Huang, H.-W. Lee, Y. Chen, C. F. Louis, J. J. Yang, *J. Biol. Chem.* **2007**, *282*, 35005–35017; d) S. R. Martin, L. Masino, P. M. Bayley, *Protein Sci.* **2000**, *9*, 2477–2488; e) D. Chin, A. R. Means, *Trends Cell Biol.* **2000**, *10*, 322–328.

[14] a) B. O. Oyajobi, *Arthritis Res. Ther.* **2007**, *9* (Supp 1), S4; b) A. Balakumaran, P. G. Robey, N. Fedarko, O. Landgren, *Expert Rev. Mol. Diagn.* **2010**, *10*, 465–480.

[15] a) W. Ji, L. Xiao, Y. Ling, C. Ching, M. Matsumoto, R. P. Bisbey, D. E. Helbling, W. R. Dichtel, *J. Am. Chem. Soc.* **2018**, *140*, 12677–12681.

[16] a) J. E. Moses, A. D. Moorhouse, *Chem. Soc. Rev.,* **2007**, *36*, 1249–1262; b) B. K. Hughes, W. A. Braunecker, D. C. Bobela, S. U. Nanayakkara, O. G. Reid, J. C. Johnson, *J. Phys. Chem. Lett.* **2016**, *7*, 3660–3665; c) S. Royuela, E. García-Garrido, M. M. Arroyo, M. J. Mancheño, M. M. Ramos, D. González-Rodríguez, Á. Somoza, F. Zamora, J. L. Segura, *Chem. Commun.,* **2018**, *54*, 8729–8732.

[17] P. Fortgang, T. Tite, V. Barnier, N. Zehani, C. Maddi, F. Lagarde, A.-S. Loir, N. Jaffrezic-Renault, C. Donnet, F. Garrelie, C. Chaix, *ACS Appl. Mater. Interfaces* **2016**, *8*, 1242–1433.

[18] J. S. Stevens, A. C. de Luca, M. Pelendritis, G. Terenghi, S. Downes, S. L. M. Schroeder, *Surf. Interface Anal.* **2013**, *45*, 1238–1246.

[19] X. Li, C. Zhang, S. Cai, X. Lei, V. Altoe, F. Hong, J. J. Urban, J. Ciston, E. M. Chan, Y. Liu, *Nat. Commun.* **2018**, *9*, 2998.

[20] J. P. Collman, N. K. Devaraj, T. P. A. Eberspacher, C. E. D. Chidsey, *Langmuir* **2006**, *22*, 2457–2464.
[21] D. L. Pavia, G. M. Lampman, G. S. Kriz, J. A. Vyvyan, *Introduction to Spectroscopy*, Cengage Learning, Belmont, **2015**, pp 52-84
[22] See Supporting Information.
[23] B. Ruan, H. Liu, L. Xie, *J. Fluoresc.* **2020**, *30*, 427–435.
[24] a) H. Pietsch, J. Tuchnitz, *Z. Phys. Chem.* **1961**, *216*, 372–374; b) N. A. Evans, *J. Soc. Dye. Colour.* **1970**, *86*, 174–177.

Entry for the Table of Contents

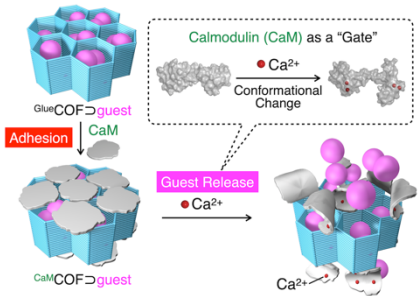

A bio-adhesive porous organic module (^{Glue}COF) carrying guanidinium ion pendants allows noncovalent accommodation of calmodulin (CaM) as a gating component onto the guest-loaded 1D nanopores (^{CaM}COF⊃guest), which release guest molecules by a conformational change of the CaM gate upon selective binding with Ca^{2+}.